

Signal Amplification Assisted by Multiple Sideband Interference in 1D Waveguide QED Systems

Kuan-Ting Lin^{1,2,*}, Ting Hsu^{1,2,3,*}, Yu-Chen Lin^{1,2}, Io-Chun Hoi⁴, and Guin-Dar Lin^{1,2,3,†}

¹*Department of Physics and Center for Quantum Science and Engineering,
National Taiwan University, Taipei 10617, Taiwan*

²*Physics Division, National Center for Theoretical Sciences, Taipei 10617, Taiwan*

³*Trapped-Ion Quantum Computing Laboratory, Hon Hai Research Institute, Taipei 11492, Taiwan*

⁴*Department of Physics, City University of Hong Kong, Hong Kong, China*

This study theoretically investigates signal amplification resulting from multiple Rabi sideband coherence in a one-dimensional waveguide quantum electrodynamical system. Specifically, we explore the behavior of a transmon while strongly driven by a coherent microwave field through a semi-infinite waveguide. To understand the underlying mechanisms of amplification, we develop a theory that explicitly takes into account multiple dressed sidebands under a strong driving field, and analyze the reflection amplitude of the probe signal. Our findings show that amplification can be related to either population inversion or multiple sideband constructive interference in some cases without population inversion. We further examine the effect of qubit dephasing during the amplification process.

I. INTRODUCTION

Accurate measurement of quantum systems plays a critical role in quantum metrology [1, 2]. During the measurement process, quantum systems inevitably experience fluctuations caused by their interaction with the surrounding environment, resulting in a noisy signal. Consequently, it is essential to consider the inherent inaccuracy of measurements due to quantum noise. A viable approach to mitigate quantum noise is through the utilization of a quantum amplifier [3–6]. The primary objective of a quantum amplifier, comprising a single atom or a group of atoms, is to enhance signal intensity and increase the signal-to-noise ratio as required. To achieve a high-gain amplifier, it is necessary for the atoms to strongly interact with the continuum modes of the electromagnetic fields. However, achieving the strong coupling regime in a three-dimensional (3D) space is challenging due to spatial mode mismatch [7–10]. By confining the radiation fields within one-dimensional (1D) waveguide systems, it is more effective to achieve perfect spatial mode matching [11–15].

In the microwave domain, the implementation of a one-dimensional (1D) waveguide system involves the interaction of superconducting artificial atoms through the guided modes of a 1D transmission line [16]. This system offers advantages in achieving strong coupling compared to real atomic systems [17]. Consequently, the 1D waveguide system serves as an excellent platform for studying various quantum-optical phenomena, including many-body entanglement [18–22], super-/sub-radiance, collective Lamb shift [23–26] and applications related to quantum communication and information [27–30]. Furthermore, the extensive research has been conducted in

the context of signal amplification, particularly when a single atom is driven by a strong coherent field [31–37]. Due to the presence of the intense driving field, the energy levels of the bare states mix to form dressed states known as Rabi sidebands [34, 38–40]. When a weak probe field resonates with the Rabi sidebands, stimulated emissions occur, resulting in amplification of the probe field. Previous studies have primarily focused on gain mechanisms that require population inversion for a specific Rabi sideband. However, amplification can still occur when the probe field is near resonance with multiple Rabi sidebands. Intuitively, it may be assumed that the emissions from each sideband with inverted population contribute independently to the gain. However, the interference between these stimulated multiple photons adds complexity to the scenario. Recently, the observation of signal amplification originating from multiple Rabi sidebands coherence has been reported [41]. Nevertheless, the physical explanation behind amplification arising from multiple Rabi sidebands in such cases remains unclear.

This research focuses on a theoretical investigation into the fundamental origin of gain in an amplifier system composed of superconducting atoms driven by a strong coherent microwave field. We consider the influence of multiple energy levels within each atom in our analysis. In our setup, the atoms can be excited from their ground state to specific excited states through a multiphoton process (driving field), resulting in amplification via stimulated emission from multiple Rabi sidebands. The primary objective is to develop a multiple sideband theory to gain insights into amplification. Our theoretical framework not only encompasses previous work on amplification with population inversion but also predicts that signal amplification can occur due to the constructive quantum interference among transitions involving multiple dressed states. Additionally, we derive a master equation that is generally valid for even many-particle cases. Through our work, we aim to pave the way for realization of a multi-atom amplifier.

* These authors contribute equally.

† guindarl@phys.ntu.edu.tw

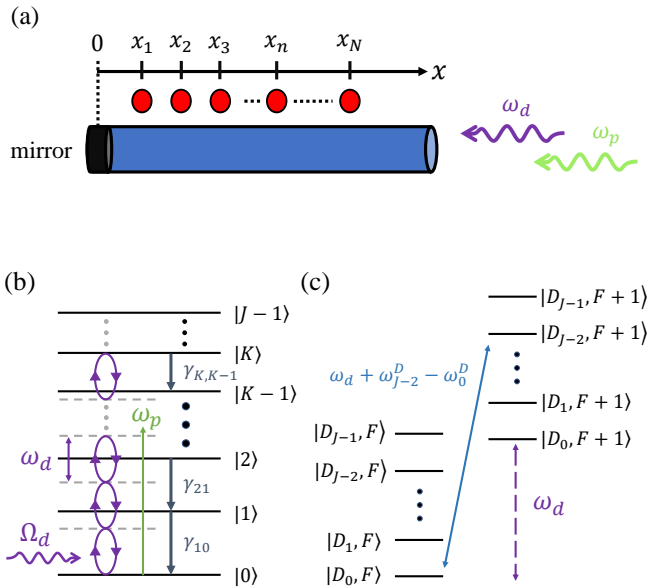


Figure 1. (a) The schematic illustrates a linear array of transmons, represented by red circles, coupled to a semi-infinite 1D waveguide. The terminated end of the waveguide acts as an antinode mirror located at $x = 0$. The coherent driving and probe fields are introduced from the opposite end to interact with the transmons. (b) A transmon with J energy levels is subjected to a strong coherent field characterized by the Rabi (carrier) frequency Ω_d (ω_d). In this case, the transmon is pumped to the state $|K\rangle$ by absorbing K photons. A weak probe beam at frequency ω_p is applied to the system. The decay rate between adjacent states $|j\rangle$ and $|j-1\rangle$ is denoted by $\gamma_{j,j-1}$. (c) The energy diagram depicts the dressed states in the rotating frame with frequency ω_d .

This paper is organized as follows. We present the theoretical model consisting of a linear chain of multiple transmons interacting with a 1D semi-infinite waveguide and derive the multiple sideband theory based on the dressed state representation in Sec. II. In Sec. III, we examine the signal amplification in single-transmon cases, considering one-, two-, and three-photon processes of the driving field, respectively, and analyze the reflection amplitude of the probe signal. Furthermore, we investigate the impact of pure dephasing on the gain behavior. Finally, we conclude our work in Sec. IV.

II. THEORY

A. Model and Hamiltonian

We consider a linear array consisting of N identical transmons, each possessing J energy levels labeled by the j th level's energy $\hbar\omega_j$ for $j = 1, 2, \dots, J$. This array is coupled to a 1D semi-infinite waveguide, with one end terminated by a perfect mirror [42], as depicted in Fig. 1(a). A strong coherent driving field is applied, charac-

terized by a Rabi frequency Ω_d and carrier frequency ω_d , entering from the open end to excite the transmons from the ground state $|0\rangle$ to an excited state $|K\rangle$ through a multiple-photon process, as illustrated in Fig. 1(b). To probe this system, we introduce a weak probe field, represented by the Rabi (carrier) frequency Ω_p (ω_p), which interacts with the light-dressed transmons. The system's Hamiltonian, denoted by $H = H_s + H_d + H_p + H_B + V$ [43–45], consists of the transmons' energy

$$H_s = \sum_{n,j} \hbar\omega_j \sigma_{jj}^n \quad (1)$$

and the field component

$$H_B = \hbar \int_0^\infty d\omega \omega a_\omega^\dagger a_\omega. \quad (2)$$

The atomic operator corresponding to the j th energy level of the n th transmon is denoted by $\sigma_{jj}^n = |j\rangle_n \langle j|$, where $n = 1, 2, \dots, N$. The operator a_ω^\dagger (a_ω) creates (annihilates) a waveguide photon with mode frequency ω , satisfying the commutation relation $[a_\omega, a_{\omega'}^\dagger] = \delta(\omega - \omega')$.

The interaction Hamiltonian is given by

$$V = i\hbar \sum_{n,j} \int_0^\infty d\omega \sqrt{j} g(\omega) \cos(k_\omega x_n) \sigma_{j,j-1}^n a_\omega + \text{H.c.} \quad (3)$$

In this expression, $\sigma_{j,j-1}^n = |j\rangle_n \langle j-1|$ represents the atomic ladder operator for the n th transmon located at position $x = x_n$. The coupling strength $\sqrt{j} g(\omega)$ describing the interaction between the j th energy level and continuous radiation field mode of frequency ω [46]. The phase experienced by the n th transmon due to the presence of the antinode mirror at $x = 0$ is given by $\cos(k_\omega x_n)$ [15, 25], where $k_\omega = \omega/v_g$ represents the wavenumber with the speed of light v_g . H.c. stands for the Hermitian conjugate. The driving and probe fields coupling to this transmon array are described by the Hamiltonians [47],

$$H_d = \hbar \sum_{n,j} \frac{\sqrt{j} \Omega_d \cos(k_d x_n)}{2} (\sigma_{j,j-1}^n e^{-i\omega_d t} + \text{H.c.}) \quad (4)$$

and

$$H_p = \hbar \sum_{n,j} \frac{\sqrt{j} \Omega_p \cos(k_p x_n)}{2} (\sigma_{j,j-1}^n e^{-i\omega_p t} + \text{H.c.}). \quad (5)$$

Here, $k_d = \omega_d/v_g$ ($k_p = \omega_p/v_g$) represents the wavenumber for the driving (probe) field.

By following the standard approach of tracing over the photonic degrees of freedom [15, 48], we obtain the Born-Markov master equation in the rotating frame with frequency ω_d as follows:

$$\begin{aligned}
\frac{d\rho}{dt} = & i \sum_{n,j} (j\omega_d - \omega_j) [\sigma_{jj}^n, \rho] \\
& + i \sum_{n,j} \frac{\sqrt{j}\Omega_d \cos(k_d x_n)}{2} ([\sigma_{j,j-1}^n, \rho] - \text{H.c.}) \\
& + i \sum_{n,j} \frac{\sqrt{j}\Omega_p \cos(k_p x_n)}{2} ([\sigma_{j,j-1}^n, \rho] e^{i(\omega_d - \omega_p)t} - \text{H.c.}) \\
& + i \sum_{nm,jl} \sqrt{j}l \Delta_{j,j-1}^{nm} ([\sigma_{j-1,j}^m, \sigma_{l,l-1}^n] - \text{H.c.}) \\
& + \sum_{nm,jl} \frac{\sqrt{j}l \gamma_{j,j-1}^{nm}}{2} ([\sigma_{j-1,j}^m \rho, \sigma_{l,l-1}^n] + \text{H.c.}) \\
& + \sum_{n,j} \gamma_{n,j}^\phi ([\sigma_{jj}^n, \sigma_{jj}^n] + \text{H.c.})
\end{aligned} \tag{6}$$

Here, the collective decay rate and Lamb shift [15, 49, 50], accounting for the dipole-dipole interaction, are given by

$$\gamma_{j,j-1}^{nm} = \frac{\gamma_{j,j-1}}{2} \text{Re} \left(e^{ik_{j,j-1}(x_n+x_m)} + e^{ik_{j,j-1}|x_n-x_m|} \right) \tag{7}$$

$$\Delta_{j,j-1}^{nm} = \frac{\gamma_{j,j-1}}{4} \text{Im} \left(e^{ik_{j,j-1}(x_n+x_m)} + e^{ik_{j,j-1}|x_n-x_m|} \right), \tag{8}$$

where $\gamma_{j,j-1} = 2\pi g^2 (\omega_j - \omega_{j-1})$ represents the bare decay rate evaluating at transition frequency $(\omega_j - \omega_{j-1})$, $k_{j,j-1} = (\omega_j - \omega_{j-1})/v_g$ is the wavenumber and Re (Im) denotes the real (imaginary) part. The last term in the master equation, Eq. (6), is added to account for the pure dephasing process. It involves the dephasing rate $\gamma_{n,j}^\phi$ for the j th level of n th transmon, and ρ is reduced density matrix of the system.

B. Reflection amplitude: perturbative analysis

In our setup, we send in a probe field from the open end to investigate the amplification process by analyzing the reflection amplitude. The reflection amplitude is denoted by $r = \left| \frac{\langle a_{\text{out}}(t) \rangle}{\langle a_{\text{in}}(t) \rangle} \right|$ with the photonic operator $a_{\text{out}}(t)$ ($a_{\text{in}}(t)$) representing the output (input) signal. The output signal then can be determined through the input one and the atomic response via the input-output relation [24, 51],

$$a_{\text{out}}(t) = a_{\text{in}}(t) + \sum_{n,j} \sqrt{j\gamma_{j,j-1}} \cos(k_{j,j-1}x_n) \sigma_{j-1,j}^n(t). \tag{9}$$

When a single-mode classical probe field is applied as input signal, the photonic operator $a_{\text{in}}(t)$ can be replaced by [52, 53]

$$a_{\text{in}} \rightarrow \frac{i\Omega_p}{2\sqrt{\frac{\omega_p}{(\omega_1 - \omega_0)}\gamma_{10}}} e^{-i\omega_p t}. \tag{10}$$

In this case, the reflection amplitude in the rotating frame with frequency ω_d is given by

$$r = \left| 1 + \frac{2i \sum_{n,j} \tilde{\gamma}_j(x_n) \langle \tilde{\sigma}_{j-1,j}^n(t) \rangle e^{i(\omega_p - \omega_d)t}}{\Omega_p} \right|, \tag{11}$$

where $\tilde{\sigma}_{j-1,j}^n(t) = \sigma_{j-1,j}^n(t) e^{i\omega_d t}$ represents a slowly-varying atomic ladder operator and $\tilde{\gamma}_j(x_n) = \sqrt{j\omega_p \gamma_{10} \gamma_{j,j-1} / (\omega_1 - \omega_0)} \cos(k_{j,j-1}x_n)$. In this study, the probe field is sufficiently weak ($\Omega_p/\gamma_{10} \ll 1$), allowing us to approximate the reduced density matrix ρ as

$$\rho(t) \approx \rho^{(0)}(t) + \frac{\Omega_p}{\gamma_{10}} \rho^{(1)}(t) e^{-i(\omega_p - \omega_d)t}, \tag{12}$$

where the expectation value is determined using $\langle \tilde{\sigma}_{j-1,j}^n(t) \rangle = \text{Tr}(\tilde{\sigma}_{j-1,j}^n \rho^{(1)}(t))$. It is noteworthy that the dynamics for the density operators $\rho^{(0)}$ and $\rho^{(1)}$ can be obtained by substituting Eq. (12) into Eq. (6).

C. Multiple sidebands theory

In this section, we present a formalism that addresses the underlying mechanism of signal amplification using the concept of dressed states, i.e., the Rabi sidebands [34]. We start with the Hamiltonian, $H_{LD} = H_D + H_L$, that describes the coherent coupling between light and the transmon system. The atomic part reads

$$\begin{aligned}
H_D = & \sum_{n,j} \hbar(\omega_j - j\omega_d) \sigma_{jj}^n \\
& - \sum_{n,j} \hbar \frac{\sqrt{j}\Omega_d \cos(k_d x_n)}{2} (\sigma_{j,j-1}^n + \sigma_{j-1,j}^n)
\end{aligned} \tag{13}$$

and the field part is given by

$$H_L = \hbar\omega_d b^\dagger b. \tag{14}$$

In this expression, the photonic operator b (b^\dagger) corresponds to the annihilation (creating) of a photon in the driving field, with energy $\hbar\omega_d$. Next, we determine the eigenstate $|D_\mu, F\rangle$ associated with eigenenergy $\hbar(\omega_\mu^D + F)$, as depicted in Fig. 1(c). This is achieved by solving the eigenequation:

$$\begin{aligned}
H_{LD} |D_\mu, F\rangle = & H_D |D_\mu\rangle \otimes H_L |F\rangle \\
= & \hbar(\omega_\mu^D + F\omega_d) |D_\mu, F\rangle.
\end{aligned} \tag{15}$$

Here, F represents the photon number, and the reflection amplitude can be rewritten as

$$r = \left| 1 + 2i \sum_{\mu\nu} C_{D_\mu D_\nu} \langle \sigma_{D_\mu D_\nu}(t) \rangle \right|. \tag{16}$$

The coefficient $C_{D_\mu D_\nu}$ is related to the atomic ladder operator through

$$C_{D_\mu D_\nu} = \sum_{n,j} \frac{\tilde{\gamma}_j(x_n)}{\gamma_{10}} \text{Tr}(\sigma_{j-1,j}^n \sigma_{D_\nu D_\mu}), \tag{17}$$

where $\sigma_{D_\nu D_\mu} = |D_\nu\rangle\langle D_\mu| = \sigma_{D_\mu D_\nu}^\dagger$ and its dynamics are determined through the optical Bloch equations:

$$\begin{aligned} \frac{d\langle\sigma_{D_\mu D_\nu}\rangle}{dt} &= \frac{d\langle D_\nu|\rho^{(1)}|D_\mu\rangle}{dt} = (i\delta_{\mu\nu}^D + \Gamma_{\mu\nu}^D)\langle\sigma_{D_\mu D_\nu}\rangle \\ &+ i\sum_q\left(\Omega_{q\nu}^D\langle\sigma_{D_\mu D_q}\rangle_{(0)} - \Omega_{\mu q}^D\langle\sigma_{D_q D_\nu}\rangle_{(0)}\right) \\ &+ \sum_{p\neq\mu, q\neq\nu}\bar{\Gamma}_{q\nu\mu p}^D\langle\sigma_{D_p D_q}\rangle - \sum_{q, p\neq\nu}\Gamma_{q\nu p q}^{D+}\langle\sigma_{D_\mu D_p}\rangle - \sum_{p, q\neq\mu}\Gamma_{pq\mu p}^{D-}\langle\sigma_{D_q D_\nu}\rangle \end{aligned} \quad (18)$$

Here, $\delta_{\mu\nu}^D = \omega_p - (\omega_\nu^D - \omega_\mu^D + \omega_d)$ denotes the detuning and the relaxation rate is expressed as $\Gamma_{\mu\nu}^D = \bar{\Gamma}_{\nu\nu\mu\mu}^D - \sum_p(\Gamma_{p\nu\nu p}^{D+} + \Gamma_{p\mu\mu p}^{D-})$ with

$$\begin{aligned} \bar{\Gamma}_{abcd}^D &= \sum_{nm, jk}\chi_{jk}^{nm}\text{Tr}[\sigma_{k-1, k}^m\sigma_{D_a D_b}]\text{Tr}[\sigma_{j, j-1}^n\sigma_{D_c D_d}] \\ &+ 2\sum_{n, j}\gamma_{n, j}^\phi\text{Tr}[\sigma_{jj}^n\sigma_{D_a D_b}]\text{Tr}[\sigma_{jj}^n\sigma_{D_c D_d}] \end{aligned} \quad (19)$$

and

$$\begin{aligned} \Gamma_{abcd}^{D\pm} &= \sum_{nm, jk}\eta_{nm, jk}^\pm\text{Tr}[\sigma_{j, j-1}^n\sigma_{D_a D_b}]\text{Tr}[\sigma_{k-1, k}^m\sigma_{D_c D_d}] \\ &+ \sum_{n, j}\gamma_{n, j}^\phi\text{Tr}[\sigma_{jj}^n\sigma_{D_a D_b}]\text{Tr}[\sigma_{jj}^n\sigma_{D_c D_d}] \end{aligned} \quad (20)$$

where $\chi_{jk}^{nm} = \sqrt{jk}\left(\frac{\gamma_{k, k-1}^{nm} + \gamma_{j, j-1}^{nm}}{2} - i(\Delta_{k, k-1}^{nm} - \Delta_{j, j-1}^{nm})\right)$ and $\eta_{nm, jk}^\pm = \sqrt{jk}\left(\frac{\gamma_{k, k-1}^{nm}}{2} \pm i\Delta_{k, k-1}^{nm}\right)$. Additionally, the second term on the right hand side describes the optical pumping process with the strength $\Omega_{ab}^D\langle\sigma_{D_a D_b}\rangle_{(0)} = \sum_{n, j}\frac{\sqrt{j}\gamma_{10}}{2}\cos(k_p x_n)\text{Tr}[\sigma_{j, j-1}^n\sigma_{D_a D_b}]\text{Tr}[\rho^{(0)}|D_b\rangle\langle D_a|]$ and the remaining terms denote the coupling between dressed states.

To elucidate the gain mechanism, we examine a rep-

resentative case with $N = 1$ hereafter. In this scenario, when the probe field resonates with a single Rabi sideband while neglecting all other sidebands, we derive the steady-state value of

$$\langle\sigma_{D_\mu D_\nu}\rangle \approx \frac{i\Omega_{\mu\nu}^D P_{\nu\mu}^D}{\Gamma_{\mu\nu}^D}, \quad (21)$$

where $P_{\nu\mu}^D = \langle\sigma_{D_\nu D_\nu}\rangle_{(0)} - \langle\sigma_{D_\mu D_\mu}\rangle_{(0)}$. The cross terms associated with optical pumping can be neglected when the driving power is sufficiently high [34]. It is observed that the population difference significantly impacts the reflection amplitude r , indicating that signal amplification can occur due to population inversion when both $\Omega_{\mu\nu}^D$ and $\Gamma_{\mu\nu}^D$ are real. The amplification resulting from population inversion has been extensively studied in previous works [31, 32, 34, 54]. However, this represents only part of the story. In our approach, several high levels of the transmon are mixed, resulting in the production of several nearly resonant Rabi sidebands. When ω_p is close to resonance with M sidebands, $\delta_{\mu\alpha\nu\beta}^D \leq \gamma_{10}$ for $\alpha, \beta = 1, 2, \dots, M$, these M sidebands must contribute to the reflection signal. To elucidate the signal amplification arising from multiple Rabi sideband coherence, we consider a simplified case with $M = 2$. According to equation (16) and equation (18), the reflection signal is determined through the following coupled equations:

$$\begin{bmatrix} \Gamma_{\mu_1\nu_1}^D + i\delta_{\mu_1\nu_1}^D & \Gamma_{\nu_2\nu_1\mu_1\mu_2}^D \\ \Gamma_{\nu_1\nu_2\mu_2\mu_1}^D & \Gamma_{\mu_2\nu_2}^D + i\delta_{\mu_2\nu_2}^D \end{bmatrix} \begin{bmatrix} \langle\sigma_{D_{\mu_1} D_{\nu_1}}\rangle \\ \langle\sigma_{D_{\mu_2} D_{\nu_2}}\rangle \end{bmatrix} = \begin{bmatrix} i\sum_q\left(\Omega_{\mu_1 q}^D\langle\sigma_{D_q D_{\nu_1}}\rangle_{(0)} - \Omega_{q\nu_1}^D\langle\sigma_{D_{\mu_1} D_q}\rangle_{(0)}\right) \\ i\sum_q\left(\Omega_{\mu_2 q}^D\langle\sigma_{D_q D_{\nu_2}}\rangle_{(0)} - \Omega_{q\nu_2}^D\langle\sigma_{D_{\mu_2} D_q}\rangle_{(0)}\right) \end{bmatrix}. \quad (22)$$

Here, the non-diagonal terms describe the mutual interaction between the Rabi sidebands. We observe that correlations between the transitions of dressed states are established, and the interference effect plays a crucial role in the reflection amplitude. These findings, which were neither observed nor predicted in previous works, have recently been confirmed through experimental observa-

tions [41]. Our work introduces a new mechanism for producing signal amplification by manipulating atomic states.

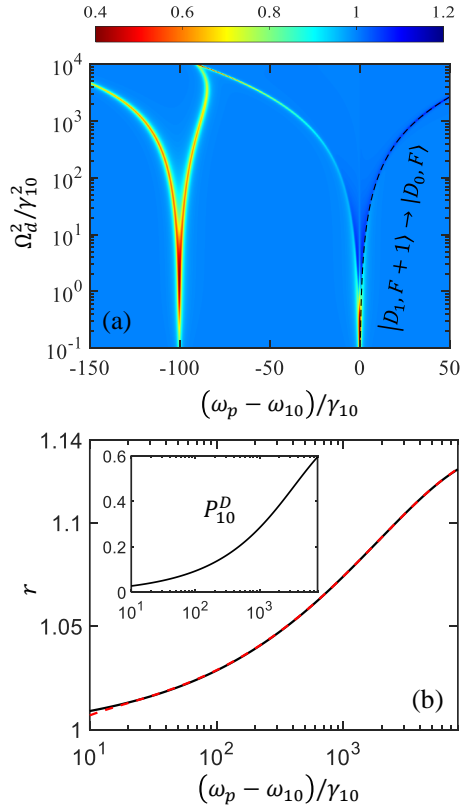


Figure 2. (a) The reflection amplitude for various driving powers Ω_d^2/γ_{10}^2 and probe frequencies ω_p . The transition frequency corresponds to the Rabi sideband $|D_1, F+1\rangle \leftrightarrow |D_0, F\rangle$ is indicated by the black dash line. In this simulation, we set $J = 6$ and use the decay rates $\gamma_{n,n-1} = n\gamma_{10}$ and the transmon energy $\hbar\omega_n = n\hbar\omega_{10} - \frac{n(n-1)}{2}\alpha$, where the frequency $\omega_{10} = 2100\gamma_{10}$, the anharmonicity $\alpha = 100\gamma_{10}$ and $n = 1, 2, \dots, 5$. (b) The reflection amplitude for the Rabi sideband $|D_1, F+1\rangle \leftrightarrow |D_0, F\rangle$. The amplitude r is computed using Eq. (23) and indicated by the black curve, which exhibits agreement with the numerical calculations represented by the red dashed curve. The inset illustrates the population difference $P_{10}^D = \langle \sigma_{D_1 D_1} \rangle_{(0)} - \langle \sigma_{D_0 D_0} \rangle_{(0)}$

III. RESULTS

A. One-photon process

We initiate our discussion by examining a simple case involving a one-photon process, achieved by setting the frequency $\omega_d = \omega_{10} = \omega_1 - \omega_0$. Figure 2(a) illustrates the dependence of the reflection amplitude on the driving power and probe frequency. In a case when $\Omega_d^2/\gamma_{10}^2 \leq 10^0$, we observe two bright stripes associated with $|0\rangle \leftrightarrow |1\rangle$ and $|1\rangle \leftrightarrow |2\rangle$ transitions, occurring at frequencies $\omega_p = \omega_{10}$ and $\omega_p - \omega_{10} = -100\gamma_{10}$, respectively. When $10^0 \leq \Omega_d^2/\gamma_{10}^2 \leq 10^1$, the signal representing the $|0\rangle \leftrightarrow |1\rangle$ transition splits into two branches, indicating the mixing of bare states to form Rabi sidebands. We also observe reflection amplitude $r > 1$, signifying amplification of the

probe field, along a single Rabi sideband associated with the $|D_1, F+1\rangle \leftrightarrow |D_0, F\rangle$ transition when $\Omega_d^2/\gamma_{10}^2 \geq 10^1$.

In order to analyze the gain mechanism, we compute the reflection amplitude for this sideband transition using

$$r = \left| 1 - \frac{2C_{01}\Omega_{01}^D}{\Gamma_{01}^D} P_{10}^D \right| \quad (23)$$

as shown by black curve in Fig. 2(b). Additionally, we present the numerical calculation of the amplitude r (red dash line) through Eq. (11) for comparison. We observe excellent agreement between our theory and the numerical results, suggesting that the incident probe field triggers stimulated emission of this Rabi sideband, leading to signal amplification. In this case, the gain is determined by population inversion [31, 34, 54].

B. Multi-photon process

We now turn to examine the reflection amplitude for the multiple photon process by setting $\omega_d = (\omega_K - \omega_0)/K$. In this section, we mainly focus on exploring the underlying gain mechanism for both of $K = 2$ and $K = 3$ cases.

Figure 3(a) displays the reflection amplitude for the $K = 2$ case. Firstly, when $\omega_p > \omega_{10}$ and $\Omega_d^2/\gamma_{10}^2 \geq 5 \times 10^2$, we observe two distinct reflection signals indicating amplification. Each signal corresponds to a specific Rabi sideband, where the gain can be attributed to population inversion, as discussed in previous section. Furthermore, within the region of $2 \times 10^1 \leq \Omega_d^2/\gamma_{10}^2 \leq 2 \times 10^2$, amplification can also occur when the two Rabi sidebands, $|D_0, F+1\rangle \leftrightarrow |D_1, F\rangle$ and $|D_3, F+1\rangle \leftrightarrow |D_1, F\rangle$, overlap. When $\Omega_d^2/\gamma_{10}^2 = 10^2$, we find that both Rabi sidebands exhibit a population difference with $P_{01}^D < 0$ and $P_{31}^D < 0$, as shown in Fig. 3(c), revealing a new mechanism for the amplification as a consequence of constructive interference between the multiple Rabi sidebands. To understand this phenomenon, we can consider a simplified model where these two Rabi sidebands originate from a V-type three-state system consisting of two excited states, $|e_1\rangle = |D_0, F+1\rangle$, $|e_2\rangle = |D_3, F+1\rangle$, and a common ground state, $|g\rangle = |D_1, F\rangle$. In this case, the dressed V-type system induces collective emission of photons, described by the collective operator $\sigma_c^- = |g\rangle\langle e_1| + |g\rangle\langle e_2|$, resulting in enhanced photon intensity due to constructive interference [55–58].

To analyze the situation, we calculate the reflection amplitude for the $M = 2$ case through Eq. (22) as shown in Fig. 3(b). It is observed that gain can be achieved within a certain window, characterized by the natural linewidth γ_{10} . Our calculations demonstrate that a 10% gain can be attained without population inversion in this setup. Moreover, this gain is greater than the previous predictions, which considered population inversion and only took into account three energy levels of an emitter [31]. These findings indicate that achieving amplification

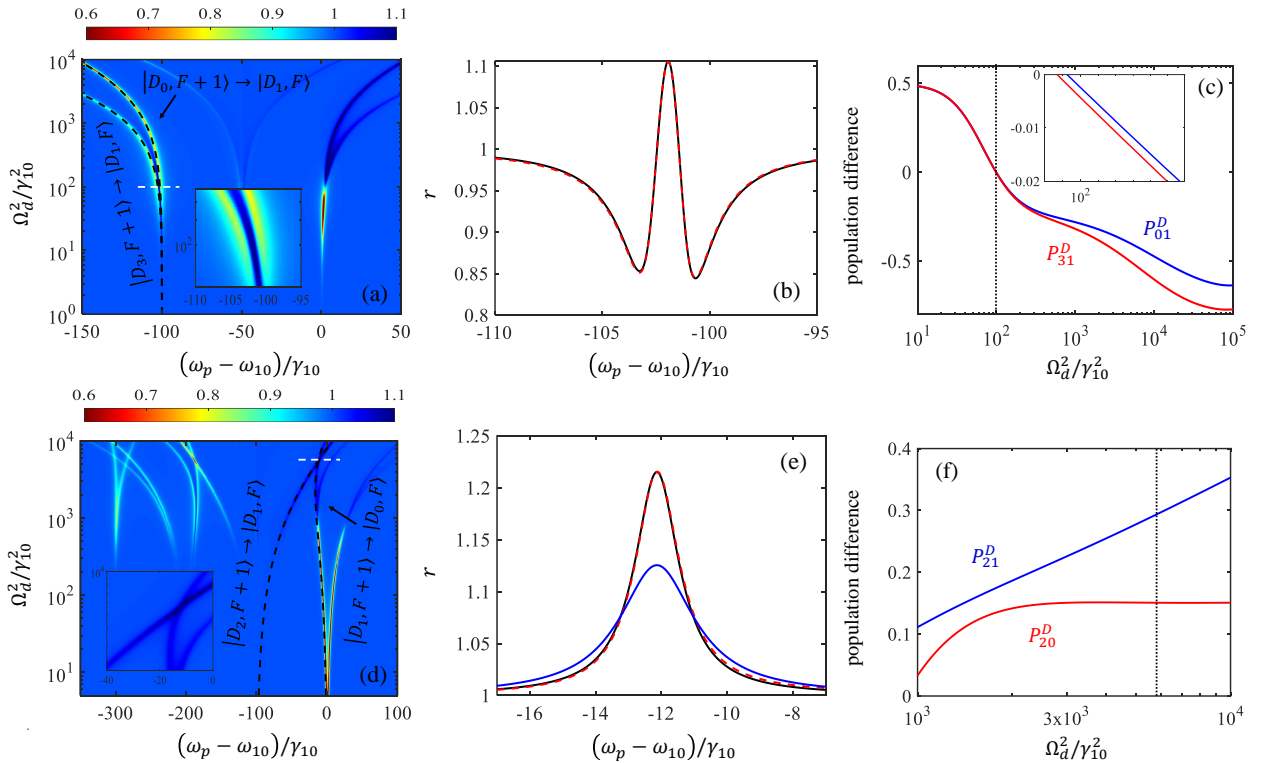


Figure 3. (a)(d) The reflection amplitudes r as a function of the driving power Ω_d^2/γ_{10}^2 and the probe frequency ω_p for $K = 2$ and $K = 3$ cases. The Rabi sideband transitions are denoted by black dash lines and zoomed-in views around the amplifications are displayed in the insets. (b)(e) Linecut plots are extracted from figure (a) and (d), where the driving powers are set to $\Omega_d^2/\gamma_{10}^2 = 10^2$ and $\Omega_d^2/\gamma_{10}^2 = 74.7^2$, as indicated by white dashed lines. The amplitudes r computed through Eq. (22) are presented by the black curve. The blue line corresponds to the resulting reflection amplitude obtained through Eq. (24). For comparison, the reflection signals calculated numerically using Eq. (11) are depicted by red dashed curves. (c)(f) The population difference of dressed states for various driving powers Ω_d^2/γ_{10}^2 . The dotted lines correspond to the powers $\Omega_d^2/\gamma_{10}^2 = 10^2$ and $\Omega_d^2/\gamma_{10}^2 = 74.7^2$, respectively.

through multiple Rabi sideband interference requires the involvement of a greater number of high levels of the transmon.

Figure 3(d) shows the reflection amplitude for the $K = 3$ case. We observe significant amplification at the intersection point of two Rabi sidebands, namely, $|D_1, F\rangle \leftrightarrow |D_2, F+1\rangle$ and $|D_0, F\rangle \leftrightarrow |D_1, F+1\rangle$, when $\Omega_d^2/\gamma_{10}^2 = 74.7^2$. Intuitively, we initially consider that the amplification is determined independently by these two sidebands. Therefore, employing the Eq. (21), we calculate the reflection signal,

$$r = \left| 1 - \frac{2C_{12}\Omega_{12}^D}{\Gamma_{12}^D} P_{21}^D - \frac{2C_{01}\Omega_{01}^D}{\Gamma_{01}^D} P_{10}^D \right|, \quad (24)$$

represented by the blue curve in Fig. 3(e). Since the populations of both Rabi sidebands are inverted, as displayed in Fig. 3(d), a 12.5% gain is obtained at the intersection point. However, the maximum achievable gain in this setup is approximately 21.5%. This suggests that the current approach is inadequate, prompting us to consider the cross-correlation of these dressed states. We then compute the amplitude r , represented by the black curve in Fig. 3(e), via Eq. (22). Our results reveal that

the gain can be further enhanced by approximately 9% through multiple sideband interference.

C. Effect of the pure dephasing process

In this section, our primary focus lies in examining the phenomenon of signal amplification within a realistic setting, specifically considering the influence of pure dephasing in cases where $K = 2$ and $K = 3$. When the dephasing rate $\gamma^\phi/\gamma_{10} \rightarrow 0$, we observe the maximum amplifications of the probe field as shown in Fig. 4. However, as the dephasing rate increases, we find that the reflection signal amplitudes decrease for both $K = 2$ and $K = 3$ cases. This observation indicates that pure dephasing can deteriorate the multiple sideband interference, resulting in a reduction in the intensity of the probe field. Consequently, our findings suggest that a high-coherence transmon is essential for achieving significant signal amplification.

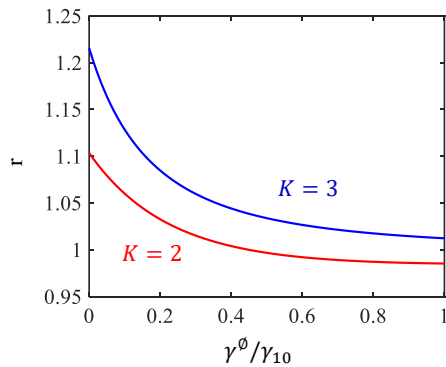


Figure 4. The reflection amplitudes for different dephasing rates for both the $K = 2$ and $K = 3$ cases. Specifically, the amplitude r is evaluated at a driving power $\Omega_d^2/\gamma_{10}^2 = 10^2$ and a probe frequency $\omega_p = \omega_{10} - 102\gamma_{10}$ for the $K = 2$ case and a driving power $\Omega_d^2/\gamma_{10}^2 = 74.7^2$ and a probe frequency $\omega_p = \omega_{10} - 12.13\gamma_{10}$ for the $K = 3$ case.

IV. CONCLUSION

In conclusion, our investigation focused on the gain mechanism of a signal amplifier composed of a multiple-level transmon driven by a strong coherent field. This intense field mixes with high levels of the transmon, forming multiple dressed states, i.e., Rabi sidebands. Through the interaction of a weak probe field, we observed a significant amplification of the probe signal. To elucidate the

gain mechanism, we developed a comprehensive theory that incorporated the dressed-state representation and took into account cross-sideband coherences. We show that amplification can be related to either population inversion or stimulated photon constructive interference involving multiple sidebands. For instance, in the two-photon case, we achieved amplification without the need for population inversion; in the three-photon scenario, the gain was further enhanced by the multiple sideband interference, in addition to the contribution due to population inversion. Remarkably, our calculations are in excellent agreement with recent experimental observations [41], ensuring the validity of our theory. We also investigated the impact of pure dephasing on the gain. Overall, our findings offer valuable insights into the mechanisms of amplification at the single-atom level and establish a solid foundation for the development of quantum repeaters, interfaces, and networks, advancing quantum communications.

ACKNOWLEDGMENTS

K.-T. L. acknowledges Chen-Yu Lee and Chun-Chi Wu for the helpful discussions and the support from the National Science and Technology Council of Taiwan under Grant No. 112-2811-M-002-067. G.-D. L. acknowledges the support from the National Science and Technology Council of Taiwan under Grant No. 112-2112-M-002-001.

-
- [1] V. Giovannetti, S. Lloyd, and L. Maccone, *Nature Photonics* **5**, 222 (2011).
 - [2] D. S. Simon, G. Jaeger, and A. V. Sergienko, *Quantum Metrology, Imaging, and Communication* (Springer International Publishing, 2017).
 - [3] S. Colombo, E. Pedrozo-Peñafiel, A. F. Adiyatullin, Z. Li, E. Mendez, C. Shu, and V. Vuletić, *Nature Physics* **18**, 925 (2022).
 - [4] X. Zuo, Z. Yan, Y. Feng, J. Ma, X. Jia, C. Xie, and K. Peng, *Physical Review Letters* **124**, 173602 (2020).
 - [5] F. Hudelist, J. Kong, C. Liu, J. Jing, Z. Ou, and W. Zhang, *Nature Communications* **5**, 10.1038/ncomms4049 (2014).
 - [6] G. Y. Xiang, T. C. Ralph, A. P. Lund, N. Walk, and G. J. Pryde, *Nature Photonics* **4**, 316 (2010).
 - [7] G. Wrigge, I. Gerhardt, J. Hwang, G. Zumofen, and V. Sandoghdar, *Nature Physics* **4**, 60 (2007).
 - [8] M. K. Tey, Z. Chen, S. A. Aljunid, B. Chng, F. Huber, G. Maslennikov, and C. Kurtsiefer, *Nature Physics* **4**, 924 (2008).
 - [9] V. Leong, M. A. Seidler, M. Steiner, A. Cerè, and C. Kurtsiefer, *Nature Communications* **7**, 10.1038/ncomms13716 (2016).
 - [10] I. Gerhardt, G. Wrigge, P. Bushev, G. Zumofen, M. Agio, R. Pfab, and V. Sandoghdar, *Physical Review Letters* **98**, 10.1103/physrevlett.98.033601 (2007).
 - [11] A. F. van Loo, A. Fedorov, K. Lalumière, B. C. Sanders, A. Blais, and A. Wallraff, *Science* **342**, 1494 (2013).
 - [12] P. Solano, P. Barberis-Blostein, F. K. Fatemi, L. A. Orozco, and S. L. Rolston, *Nature Communications* **8**, 10.1038/s41467-017-01994-3 (2017).
 - [13] F. L. Kien, S. D. Gupta, K. P. Nayak, and K. Hakuta, *Physical Review A* **72**, 10.1103/physreva.72.063815 (2005).
 - [14] Z. Liao, X. Zeng, S.-Y. Zhu, and M. S. Zubairy, *Physical Review A* **92**, 10.1103/physreva.92.023806 (2015).
 - [15] K.-T. Lin, T. Hsu, C.-Y. Lee, I.-C. Hoi, and G.-D. Lin, *Scientific Reports* **9**, 10.1038/s41598-019-55545-5 (2019).
 - [16] A. S. Sheremet, M. I. Petrov, I. V. Iorsh, A. V. Poshakinskiy, and A. N. Poddubny, *Reviews of Modern Physics* **95**, 10.1103/revmodphys.95.015002 (2023).
 - [17] X. Gu, A. F. Kockum, A. Miranowicz, Y. xi Liu, and F. Nori, *Physics Reports* **718-719**, 1 (2017).
 - [18] I. M. Mirza and J. C. Schotland, *Physical Review A* **94**, 10.1103/physreva.94.012302 (2016).
 - [19] I. M. Mirza and J. C. Schotland, *Physical Review A* **94**, 10.1103/physreva.94.012309 (2016).
 - [20] P. Facchi, M. S. Kim, S. Pascazio, F. V. Pepe, D. Pomarico, and T. Tufarelli, *Physical Review A* **94**, 10.1103/physreva.94.043839 (2016).
 - [21] G.-Z. Song, M.-J. Tao, J. Qiu, and H.-R. Wei, *Physical Review A* **106**, 10.1103/physreva.106.032416 (2022).

- [22] G.-Q. Zhang, W. Feng, W. Xiong, D. Xu, Q.-P. Su, and C.-P. Yang, arXiv 2302.06204.
- [23] J. A. Mlynek, A. A. Abdumalikov, C. Eichler, and A. Wallraff, *Nature Communications* **5**, 10.1038/ncomms6186 (2014).
- [24] K. Lalumière, B. C. Sanders, A. F. van Loo, A. Fedorov, A. Wallraff, and A. Blais, *Physical Review A* **88**, 043806 (2013).
- [25] P. Wen, K.-T. Lin, A. Kockum, B. Suri, H. Ian, J. Chen, S. Mao, C. Chiu, P. Delsing, F. Nori, G.-D. Lin, and I.-C. Hoi, *Physical Review Letters* **123**, 233602 (2019).
- [26] A. Albrecht, L. Henriët, A. Asenjo-Garcia, P. B. Dieterle, O. Painter, and D. E. Chang, *New Journal of Physics* **21**, 025003 (2019).
- [27] W.-J. Lin, Y. Lu, P. Y. Wen, Y.-T. Cheng, C.-P. Lee, K. T. Lin, K. H. Chiang, M. C. Hsieh, C.-Y. Chen, C.-H. Chien, J. J. Lin, J.-C. Chen, Y. H. Lin, C.-S. Chuu, F. Nori, A. F. Kockum, G. D. Lin, P. Delsing, and I.-C. Hoi, *Nano Letters* **22**, 8137 (2022).
- [28] V. E. Elfving, S. Das, and A. S. Sørensen, *Physical Review A* **100**, 10.1103/physreva.100.053843 (2019).
- [29] W.-K. Mok, D. Aghamalyan, J.-B. You, T. Haug, W. Zhang, C. E. Png, and L.-C. Kwек, *Physical Review Research* **2**, 10.1103/physrevresearch.2.013369 (2020).
- [30] Z. Liao and M. S. Zubairy, *Physical Review A* **98**, 10.1103/physreva.98.023815 (2018).
- [31] E. Wiegand, P.-Y. Wen, P. Delsing, I.-C. Hoi, and A. F. Kockum, *New Journal of Physics* **23**, 043048 (2021).
- [32] W.-C. Chien, Y.-L. Hsieh, C.-H. Chen, D. Dubyna, C.-S. Wu, and W. Kuo, *Optics Express* **27**, 36088 (2019).
- [33] P. Wen, A. Kockum, H. Ian, J. Chen, F. Nori, and I.-C. Hoi, *Physical Review Letters* **120**, 063603 (2018).
- [34] K. Koshino, H. Terai, K. Inomata, T. Yamamoto, W. Qiu, Z. Wang, and Y. Nakamura, *Physical Review Letters* **110**, 263601 (2013).
- [35] Y.-J. Zhao, J.-H. Ding, Z. H. Peng, and Y. xi Liu, *Physical Review A* **95**, 10.1103/physreva.95.043806 (2017).
- [36] A. Vinu and D. Roy, *Physical Review A* **101**, 10.1103/physreva.101.053812 (2020).
- [37] C. Macklin, K. O’Brien, D. Hover, M. E. Schwartz, V. Bolkhovskiy, X. Zhang, W. D. Oliver, and I. Siddiqi, *Science* **350**, 307 (2015).
- [38] J. Mompert and R. Corbalán, *Journal of Optics B: Quantum and Semiclassical Optics* **2**, R7 (2000).
- [39] J. Braumüller, J. Cramer, S. Schülz, H. Rotzinger, L. Radtke, A. Lukashenko, P. Yang, S. T. Skacel, S. Probst, M. Marthaler, L. Guo, A. V. Ustinov, and M. Weides, *Physical Review B* **91**, 10.1103/physrevb.91.054523 (2015).
- [40] G. Oelsner, P. Macha, O. V. Astafiev, E. Il’ichev, M. Grajcar, U. Hübner, B. I. Ivanov, P. Neillinger, and H.-G. Meyer, *Physical Review Letters* **110**, 10.1103/physrevlett.110.053602 (2013).
- [41] F. Aziz, K. T. Lin, P. Y. Wen, Samina, Y. C. Lin, E. Wiegand, C.-P. Lee, Y.-T. Cheng, C.-Y. Chen, C.-H. Chien, K.-M. Hsieh, Y.-H. Huang, I. Hou, J.-C. Chen, Y.-H. Lin, A. F. Kockum, G. D. Lin, and I.-C. Hoi, arXiv 2302.07442.
- [42] I.-C. Hoi, A. F. Kockum, L. Tornberg, A. Pourkabirian, G. Johansson, P. Delsing, and C. M. Wilson, *Nature Physics* **11**, 1045 (2015).
- [43] B. Peropadre, J. Lindkvist, I.-C. Hoi, C. M. Wilson, J. J. Garcia-Ripoll, P. Delsing, and G. Johansson, *New Journal of Physics* **15**, 035009 (2013).
- [44] K. Koshino and Y. Nakamura, *New Journal of Physics* **14**, 043005 (2012).
- [45] U. Dörner and P. Zoller, *Physical Review A* **66**, 10.1103/physreva.66.023816 (2002).
- [46] J. Koch, T. M. Yu, J. Gambetta, A. A. Houck, D. I. Schuster, J. Majer, A. Blais, M. H. Devoret, S. M. Girvin, and R. J. Schoelkopf, *Physical Review A* **76**, 042319 (2007).
- [47] A. F. Kockum, M. Sandberg, M. R. Vissers, J. Gao, G. Johansson, and D. P. Pappas, *Journal of Physics B: Atomic, Molecular and Optical Physics* **46**, 224014 (2013).
- [48] H. J. Carmichael, *Statistical Methods in Quantum Optics 1* (Springer Berlin Heidelberg, 1999).
- [49] R. H. Lehmann, *Physical Review A* **2**, 883 (1970).
- [50] M. Gross and S. Haroche, *Physics Reports* **93**, 301 (1982).
- [51] C. W. Gardiner and M. J. Collett, *Physical Review A* **31**, 3761 (1985).
- [52] I. Strandberg, Y. Lu, F. Quijandria, and G. Johansson, *Physical Review A* **100**, 063808 (2019).
- [53] Y. Lu, I. Strandberg, F. Quijandria, G. Johansson, S. Gasparinetti, and P. Delsing, *Physical Review Letters* **126**, 253602 (2021).
- [54] O. V. Astafiev, A. A. Abdumalikov, A. M. Zagoskin, Y. A. Pashkin, Y. Nakamura, and J. S. Tsai, *Physical Review Letters* **104**, 10.1103/physrevlett.104.183603 (2010).
- [55] G.-D. Lin and S. F. Yelin, *Physical Review A* **85**, 10.1103/physreva.85.033831 (2012).
- [56] G.-D. Lin and S. F. Yelin, in *Advances In Atomic, Molecular, and Optical Physics* (Elsevier, 2012) pp. 295–329.
- [57] A. Konovalov and G. Morigi, *Physical Review A* **102**, 10.1103/physreva.102.013724 (2020).
- [58] A. P. Orioli, J. Thompson, and A. Rey, *Physical Review X* **12**, 10.1103/physrevx.12.011054 (2022).